

---

## CHARACTERIZATION AND EVALUATION OF NATURAL ZEOLITE AS A POZZOLANIC MATERIAL

---

Mohamed El-Shahate Ismaiel Saraya,<sup>a,b,\*</sup>, Mohamed Sayed Thabet<sup>a,c</sup>

<sup>a</sup> Department of Chemistry, Faculty of Science, Al-Azhar University, P.O.11884, Nasr City, Cairo, Egypt.

<sup>b</sup> Department of Chemistry, Faculty of Science and Arts (Mikhwaha), Al-Baha University, Saudi Arabia

<sup>c</sup> Department of Chemistry, Faculty of Science, Jazan University, Saudi Arabia

\* Corresponding author, Tel.: +20 1061441312, mohamedsaraya@azhar.edu.eg

---

### ABSTRACT

*This paper presents details about mineralogical and chemical composition of natural zeolite (NZ) from Harrat Shama for using it as a pozzolanic material. The structural properties and mineralogical composition of NZ were determined using XRF, XRD, FTIR, DSC, SEM-EDX as well as study surface texture and cation exchange capacity. The geopolymer paste was prepared using sodium silicate solution as activator for zeolite and incubated at 25 and 45 °C up to 90 days. The compressive strength of NZ-based geopolymer was investigated up to 90 days. Five blended cement were designed by substitution for Portland cement by 0 %, 5 %, 10 %, 15 % and 20% of NZ. The compressive strength of NZ-OPC pastes were studied up to 90 days. The microstructure of NZ-Based geopolymer and hydrated NZ-cement pastes were tested. The results were shown that the sum of SiO<sub>2</sub>, Al<sub>2</sub>O<sub>3</sub>, and Fe<sub>2</sub>O<sub>3</sub> content in the natural zeolite was approximately 82.71.3% and mainly composed of clinoptilolite mineral. Geopolymerization of NZ gave a good dense geopolymer matrix with high early stage mechanical properties. The NZ has shown improving early stage compressive strength of all blended cement pastes up to 7 days. The incorporation of nature raw zeolite in cement, up to 10% wt, improved the compressive strength to 7-29%. Generally, Saudi Arabian natural zeolite (NZ) have high pozzolanic properties and could be used in the preparation of geopolymers matrix and blended cement pastes.*

**Keywords:** Natural raw zeolite; Characterization; Geopolymerization; Pozzolana; Saudi Arabia

### 1. INTRODUCTION

Natural zeolites are one of effective absorbents, ion-exchangers, molecular sieves which used in many applications [1]. Natural zeolites, as a cheap and locally available absorbent, were used in the energy field and their related applications were as additives, catalysts and absorbents [2, 3]. The removal of pollutants was evaluated [4-6].

Huge amounts of raw materials and energy were consuming for production of Portland cement that consider as one of the primary sources of global warming [7]. Davidovits [8] prepared a new material (geopolymer) as an alternative material for Portland cement. Geopolymer are amorphous materials prepared at ambient temperature or slightly elevated [9]. Due to the unique properties of geopolymer, it

is suitable for use in many applications such as building and construction field [8, 10]. The natural raw materials and industrial waste which are based on aluminum silicate minerals are suitable for preparing of geopolymers such as fly ash [11, 12] natural pozzolana [13], metakaolin [14]. The natural zeolite is considered as one of the suitable materials for fabrication of geopolymer. The mechanical properties of metakaolin-based geopolymer were enhanced by addition of natural zeolite as filler [15]. Bulgaria natural zeolite was activated by different alkaline activators. The results showed that the sodium silicate (water soluble glass) gave the highest compressive strength at 28 days [16]. Natural zeolite cement mortar was designed, and the result showed that the early strength was dramatically

increased and the strength at 7 days was higher than that of the OPC [17].

Pozzolana usually used to improve the physico-chemical and mechanical properties of cement pastes and concrete [18]. The pozzolana is mainly composed of silica and aluminates that have ability to react with calcium hydroxide for forming components have binding properties. These materials may be industrial by-products such as silica fume, slag and fly-ashes or natural such as vitreous pumice, diatomite earths, metakaolin and zeolitic tuffs [19, 20]. Natural zeolite (NZ) is hydrate alumino-silicates which have large quantities of reactive  $\text{SiO}_2$  and  $\text{Al}_2\text{O}_3$ . In this respect, a number of investigations were attempted to monitor the performance of NZ as supplementary cementitious materials. The engineering properties of the blended cement pastes and concrete containing natural zeolite were presented. The results of some studies showed that the replacement of cement with 20% zeolite is considered the best ratio [21, 22]. The effects of calcination temperature on the pozzolanic activity of natural zeolites were investigated. The blended cement with calcined forms of zeolite showed less water/cement ratio, improve workability of the pastes and increase the mechanical properties [23]. Burriss and Juenger [24] observed the milling of natural zeolites that used as pozzolana materials to improve the activity of zeolites. Uzal and Turanl [25] confirmed that no free  $\text{Ca}(\text{OH})_2$  in hardened pastes, containing high (above 20 %) volume of natural zeolite, at 28 days. Karakurt and Topçu [26] reported that the durability of concrete against alkali-silica reaction and sulfate effects were improved by the addition of natural zeolite as pozzolanic material. The evolution of the early hydration of cements blended with natural zeolites showed that their addition accelerates the onset of  $\text{C}_3\text{S}$  hydration and precipitation of CH and AFt [27]. Tydlitát et al [28] concluded that the addition of natural zeolite to Portland cement up to 40 % accelerates the early hydration process due to the effect of aluminate of zeolite towards the AFt-AFm conversion process. Addition 10 %

of natural zeolite to concrete has been proven to increase its density, ultrasonic pulse velocity and freeze-thaw resistance compared to that of normal concrete [29]. It was found that the concrete mixtures which contain silica fume or natural pozzolana had high resistance against chloride diffusion [30]. Addition of clinoptilolite and silica fume to cement delayed the dissolution of gypsum in the early period of hydration [31].

In King of Saudi Arabian (KSA), many of the extensive areas of aluminosilicates material deposits were not economically exploited. This is mainly related to lack of sufficient studies to illustrate their applications. Due to this fact, this study aims to characterize Harrat Shama natural raw zeolite deposits and study their potentials as raw materials for blended cement and geopolymer.

## 2. MATERIALS AND METHODS

### 2.1 Materials

The Harrat Shama (HS) is located in the western part of Saudi Arabia, about 120 km southeast of Jeddah city near to Shuaiba water desalination plant (Lat:  $20^\circ 41' 1.66$  and Long:  $39^\circ 41' 45.15$ ). It is a part of lava fields that founding in the Arabian Plate [32], (Fig. 1). Motelib et al. [33] were studied the different volcanic sequences in Harrat Shama (HS). According to their results the HS is divided into two sequences lower and upper whereas zeolite-bearing bedded tuffs were found in the lower sequence. Zeolite-bearing bedded tuff is occurred as volcanic cone and its thickness over  $\sim 30$  m. We collected a representative sample of natural zeolite (about 20 kgs) from a natural deposit at Jabal Shamah (Tuffil). The zeolite sample was ground to pass from sieve No. 200, homogenized and dried at  $100^\circ\text{C} \pm 5^\circ\text{C}$  for 24 hr.

### 2.2. Preparation of NZ- base geopolymer paste

Sodium silicate with  $\text{SiO}_2/\text{Na}_2\text{O} = 1.7$  and density  $1.68 \text{ g/cm}^3$  was employed as an activator solution. An activator/powder ratio of 0.6 was used to prepare the geopolymer paste;

it was poured into cylinder molds after mixing poured with a diameter of 2.5 cm and a height of 2.5 cm for 24 hr and then demolded. The geopolymers G-NZ1 cylinders were incubated at ambient temperature and G-NZ2 cylinders at 45 °C for 3, 7, 28, and 90 days curing times. Three cylinders were crushed in order to determine compressive strength for the geopolymer samples up to 90 days. The hardened zeolite based geopolymer cured for 28 days were investigated by XRD and FTIR, DSC and the selected samples were investigated using SEM-EDX after treatment with acetone/methanol mixture to terminate the geopolymerization process [34].

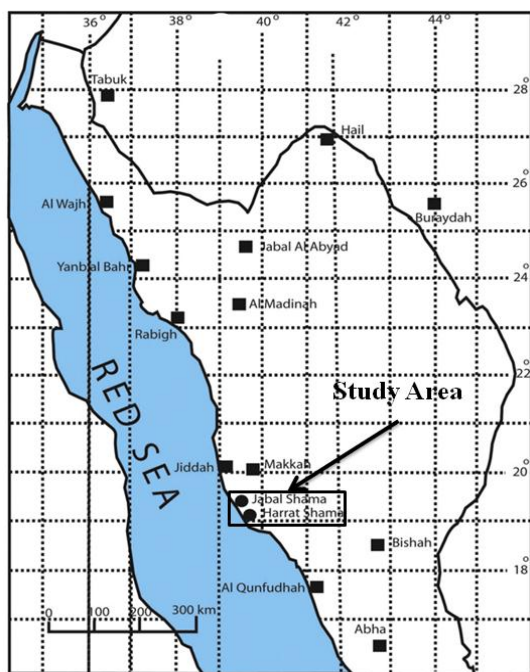


**Fig. 1.** A map of the Arabian Plate showing location of the Harrat Shama.

### 2.3. Preparing of natural zeolite blended cement

OPC type CEM I42.5 R was used to prepare blended cements of natural zeolite. The chemical composition of cement is shown in Table 1. Five blended cements were prepared by substitution of OPC (Ordinary Portland Cement) with 0, 5, 10, 15 and 20 mass % of natural raw zeolite. These blended cements

were coded as OPC, OPC-NZ5, OPC-NZ10, OPC-NZ15 and OPC-NZ20. The ingredients of each mixture were mixed in an agate mortar to homogeneity. The water/powder ratio was 0.42 in all cases. The NZBC pastes were molded into cylinder molds with an internal diameter of 2.5 cm and a height of 2.5 cm, compacted and then covered. The specimens were incubated at 25 °C and at 100% relative humidity for 24 h, and then de-molded. The hardened blended cements were kept under water up to 90 days. Three cylinders were used for determining the compressive strength at 3, 7, 28 and 90 days of curing. The compressive strength measurements were carried out using an automatic compression test machine. A commercially available, Microwave oven was used for stopping the hydration of cement pastes [35]. Some selected samples were investigated using FTIR, DSC, XRD and SEM-EDX techniques.

### 2.4. Analytical instruments

The chemical composition of zeolite sample was analyzed by X-Ray Fluorescence (XRF) (Pnalytical Axios advanced XRF). The low-temperature nitrogen adsorption/desorption isotherms (77.4 K) were determined using a surface area Quanta Chrome Nova 2000 USA. Field emission scanning electron microscopy, a JEOL JSM 6360 DLA, was used for determination the morphology of the samples. CEC of the natural zeolite was determined by ammonium acetate method as [36]. XRD patterns of natural zeolite, geopolymers and blended cement samples were recorded using An XRD 7000 (Shimadzu Instruments, Japan) at a  $2\theta$  scan speed of  $4^\circ \text{ min}^{-1}$ ,  $\lambda = 0.154 \text{ nm}$  with Cu  $K\alpha$  as a radiation source. The FTIR spectra of natural zeolite, geopolymers and blended cement samples were record using A JASCO Asia Portal - FT/IR-6300 Spectrometer. The thermal behaviour of natural zeolite, geopolymers and blended cement samples were performed on DSC (NETZSCH STA 409 C/CD instrument). The samples were investigated up

to 1000 °C using a rate of 10 °C/min in an He atmosphere.

### 3. RESULTS AND DISCUSSION

#### 3.1. Characterization of natural raw zeolite

Physical properties and chemical composition of the natural zeolite is listed in Tables 1 and 2. They indicate that the total SiO<sub>2</sub>, Al<sub>2</sub>O<sub>3</sub>, and Fe<sub>2</sub>O<sub>3</sub> contents in the zeolite is 83.19 % approximately, matching with the requirements stated in ASTM C618 [37] for a natural pozzolana. Furthermore Chakchouk et al. [38] indicated that materials having a total percentage of SiO<sub>2</sub>, Al<sub>2</sub>O<sub>3</sub>, and Fe<sub>2</sub>O<sub>3</sub> greater than 50% are suitable to produce a good pozzolanic material. It can be seen from these data that, the Si/Al ratio for NZ sample is 4.6. According to Perraki and Orfanoudaki [39] the zeolite is a clinoptilolite type [40].

Fig. 2a illustrates the XRD patterns of the raw zeolite. The XRD peaks of clinoptilolite mineral appeared at 2 $\theta$  values of 9.8°, 11.17°, 22.3°, 22.7°, 26.1°, 28.14°, 30.0° and 32.08° (JCPDS No 00-025-1349) [41]. The cowlesite mineral relates to the natrolite subgroup as a fibrous zeolite in the Dana classification, where Strunz placed it in a separate series [42]. The cowlesite has peaks at 2 $\theta$  of 5.8°, 4.46°, 19.8° and 30.07° [43] while cristobalite appeared at

2 $\theta$  of 21.7° [41]. Semi-quantitative XRD analysis shows that NZ was mainly consisted of clinoptilolite (45 wt %), cowlesite (41 wt %) and cristobalite (14 wt %).

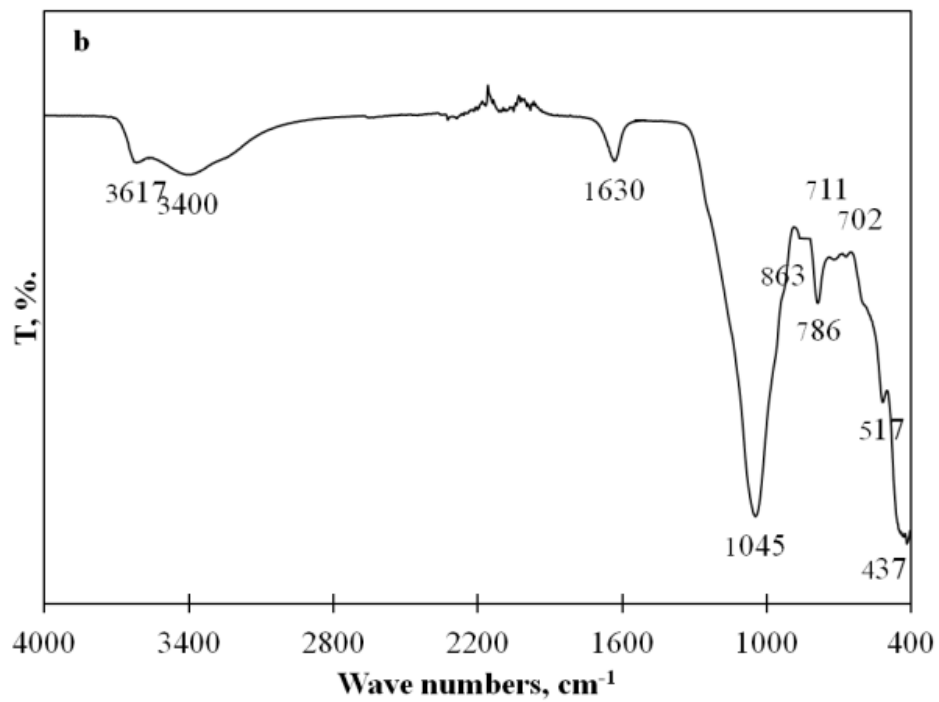
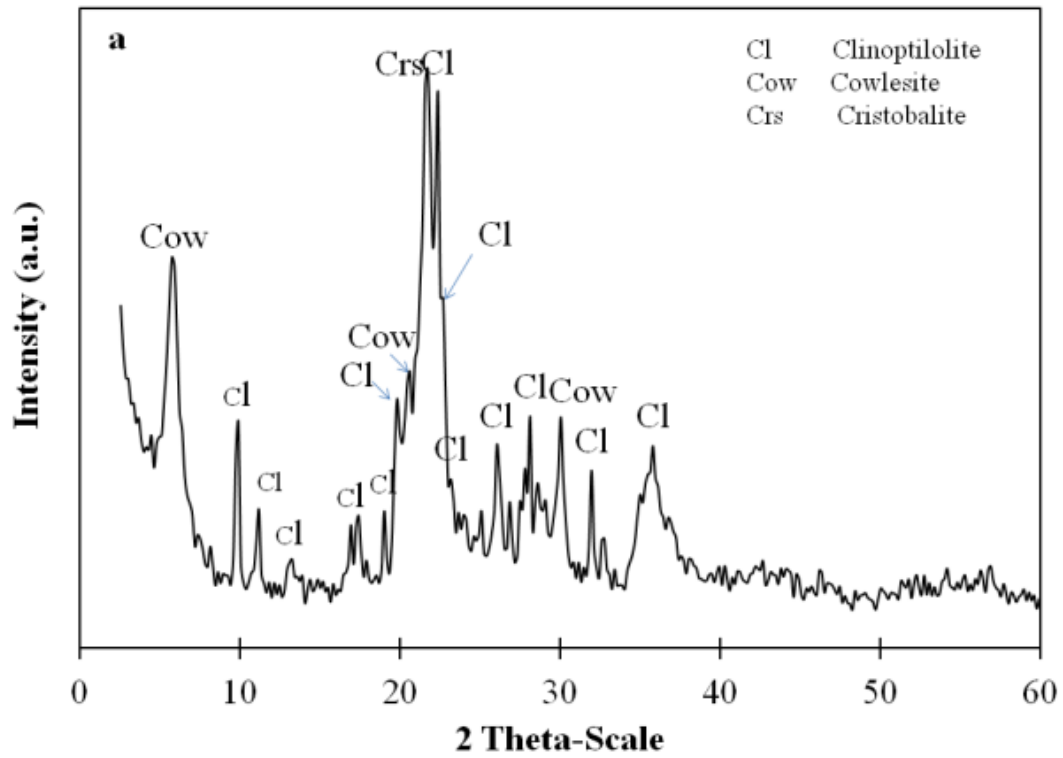
Fig. 2b shows FT-IR spectra of natural raw zeolite in the region between 400 and 4000 cm<sup>-1</sup>. The structure of zeolite can be estimated through its FTIR spectrum [44]. It is clearly shown different absorption bands at 437, 517, 786, 1045, 1630, 3400 and 3617 cm<sup>-1</sup>. The strong band at 1045 cm<sup>-1</sup> is related to the T-O stretching vibration. This band gives estimation about aluminum content in the framework of zeolite mineral, where it shifts to higher frequencies with decreasing number of Al atoms in the framework tetrahedral sites. The band at 437 cm<sup>-1</sup> is assigned to a T-O bending mode and intensity of this band is independent on the degree of crystallinity [39]. The water has several forms in zeolite structure; the band at 3617 cm<sup>-1</sup> is connected to interaction of the water hydroxyl with the cations. A band at 3400 cm<sup>-1</sup> is due to vibration of the bonds O-H...O i.e. attributed to the hydrogen bonding of the water molecule to surface oxygen, A band at 1630 cm<sup>-1</sup> is attributed to the bending mode of the water. Bands in the region 500–800 cm<sup>-1</sup> are due to pseudo-lattice vibrations and show the nature of the channel cations [40].

**Table 1: Chemical composition of natural raw zeolite and cement in mass %.**

Component	SiO <sub>2</sub>	Al <sub>2</sub> O <sub>3</sub>	CaO	K <sub>2</sub> O	MgO	Fe <sub>2</sub> O <sub>3</sub>	Na <sub>2</sub> O	SO <sub>3</sub>	TiO <sub>2</sub>	LOI	Total
NZ	66.96	15.17	3.80	2.20	1.53	1.06	0.16	-	0.08	10.2	99.40
CEM I 42.5 R	20.88	6.08	63.00	0.01	1.5	3.18	0.02	1.6	-	1.9	99.88

**Table 2: Physical properties of natural raw zeolite**

Cation-exchange capacity	2.8 meq/100 g
Specific gravity	2.1 g cm <sup>-3</sup>
Mineralogical composition	Clinoptilolite (45%), Cowlesite (41%), and Cristobalite (14%)
Particles size	100% < 43 $\mu$ m
Surface area, N <sub>2</sub> - adsorption	38.3 m <sup>2</sup> /g
Pore radius	17.39 Å
Porous volume	0.085 cc/g



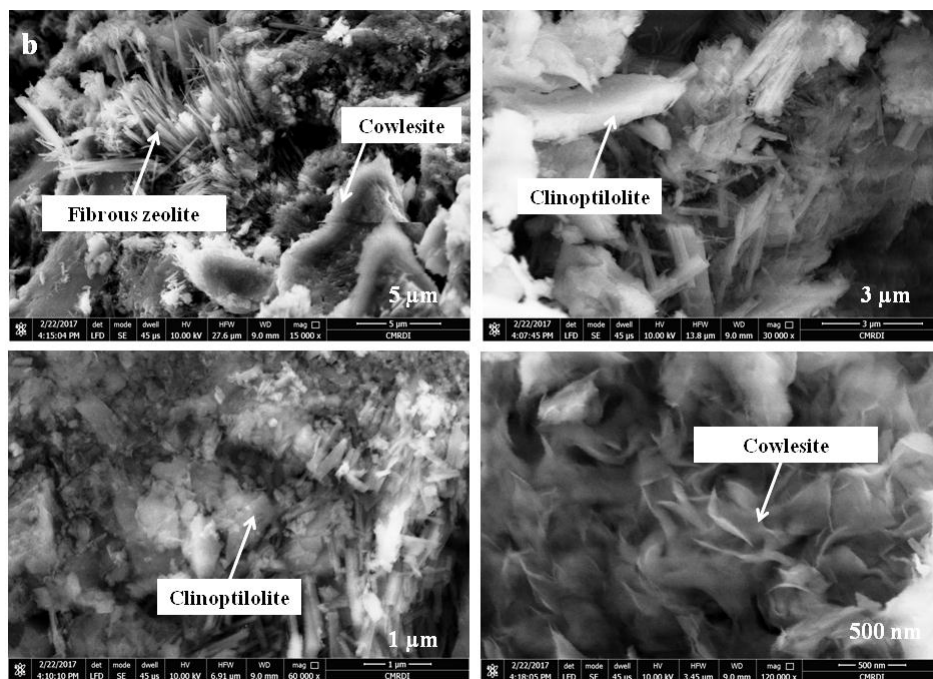
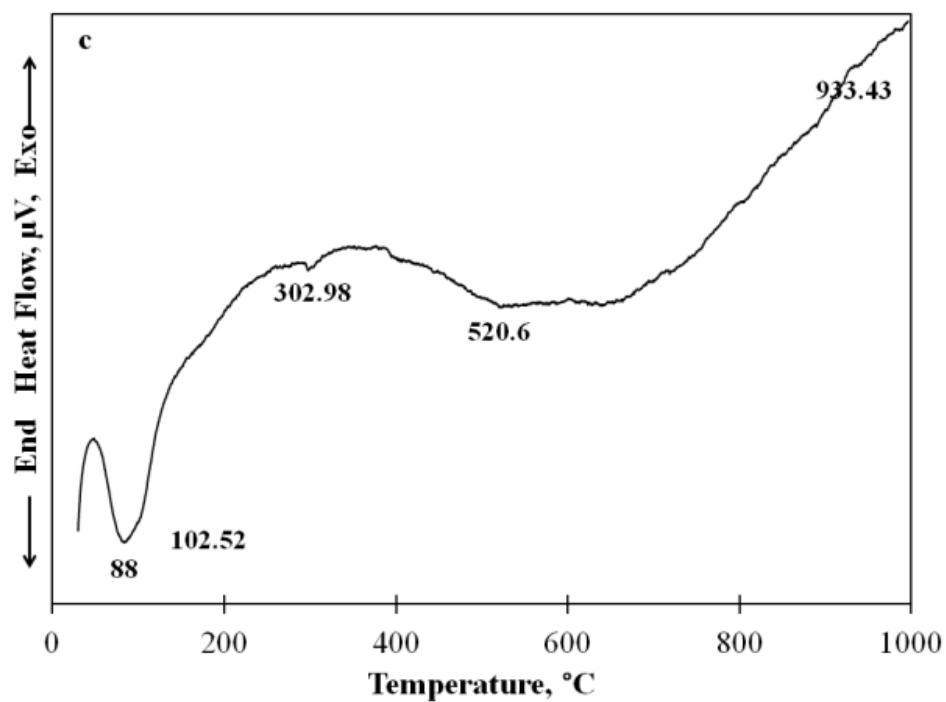


Fig. 2. (a) X-ray diffraction, (b) FTIR spectra, (c) DSC curve, (d) FESEM images of natural raw zeolites.

Fig. 2c shows the DSC curve of the natural raw zeolite. There is only one continuous water loss peak at 50 °C - 200 °C. This endothermic effect is mainly due to loss of the weakly bound water [45]. The nature of water molecules in the zeolite depends on many factors, from which number and the type of the cations in the structure of the zeolite [46]. It is no secret that the climate of Saudi Arabia is dry and very hot, affecting the water content of rocks and natural minerals. Alver et al. [47] showed that the dehydration behavior of the clinoptilolite could be controlled by the exchangeable cations and the sites occupied by cations. Fig. 2c shows the enthalpy of the water loss is 22.38 J g<sup>-1</sup> that agreement with XRD results (NZ have about 45 wt % clinoptilolite). Castaldi et al. [45] conformed the zeolite with monovalent ions has the lowest loss of weakly bound water than polyvalent. As seen from Fig. 2c there is no apparent endothermic peaks at 450 °C [48]. This assures that the sample consists mainly of clinoptilolite mineral whereas heulandite is thermally unstable and undergoes structural collapse below 450 °C [47]. A weak endothermic effect in the temperature range of 440–580 °C is related to dehydroxylation process of the surface OH groups [49]. The endothermic effects at 302 °C and 520 °C are related to the distortions of the framework structure of cowlesite due to dehydration process. The morphology of natural zeolite was investigated by FESEM and the corresponding images are shown in Fig. 2d. There are three different structural variations. The flattened platy or tabular crystals are typical of the clinoptilolite zeolite while cowlesite mineral appears as hemispheres of delicate with very thin blades. Also, there are chain-like structures whose minerals form acicular or needle-like prismatic crystals related to cowlesite of other fibrous zeolite minerals [50].

### 3.2. Characterization of NZ-based geopolymer paste

A photograph of NZ-based geopolymer is shown in Fig. 3a. The results for compressive strength of NZ based geopolymers (each

sample was triplicated) as a function of time and curing temperature are illustrated in Fig. 3b. Geopolymer samples were coded as G-NZ1 and G-NZ2 with respect to the curing temperature at ambient and 45 °C, respectively. It can be seen that the prepared zeolite geopolymers have increasing compressive strength with curing time up to 90 days. Both samples show slight increase in compressive strength in the first week of curing and enhanced sharply after this period up to 28 days. The geopolymer sample that cured at 45 °C shows a greater compressive strength than that cured at room temperature up to 90 days. This is due to the effect of temperature on enhancing the interaction between activated solution and zeolite, resulting in increased reaction products and improved mechanical properties [18].

Fig. 3c shows the XRD patterns of NZ - based geopolymer cured for 3 and 28 days at an ambient temperature and 45 °C. It is obvious that changes in mineralogical composition of NZ with curing time and temperature and the enhanced halo pattern between 2 $\theta$  18° and 38° indicates presence of amorphous nature of geopolymer [22]. At 3 days of curing the crystalline phases of zeolite dominate in their XRD patterns for both samples cured at ambient temperature and 45 °C, while peak intensities of these mineral became slightly higher at 45 °C. The peak observed with d-spacing value of 15.2 Å, which correspond to cowlesite and peak with d-space 4.089 Å which related to cristobalite in raw zeolite, totally disappeared. This indicated dissolution in geopolymeric reaction [16].

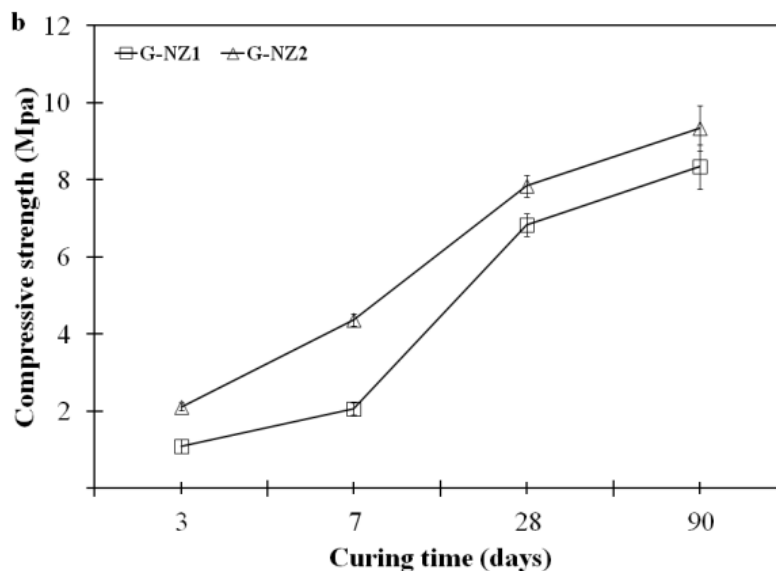
The FTIR spectra of NZ-base geopolymer are shown in Fig. 3d. The peaks in the range 950–1222 cm<sup>-1</sup> may be related to asymmetric stretching vibration band of Si-O-Si and Al-O-Si. In this study it is assumed the formation of aluminosilicate gel [51]. The peak was observed at 790 cm<sup>-1</sup> which may refer to symmetric stretching vibration of Si-O-Si. However, peak at 468 cm<sup>-1</sup> attribute to the bending vibrations Si-O-Si and O-Si-O. The

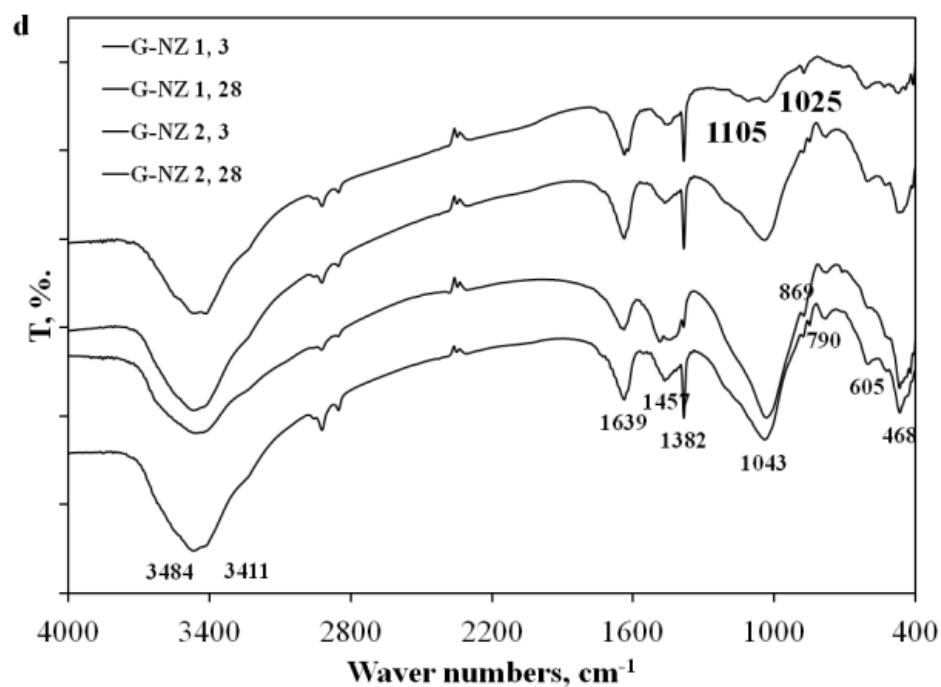
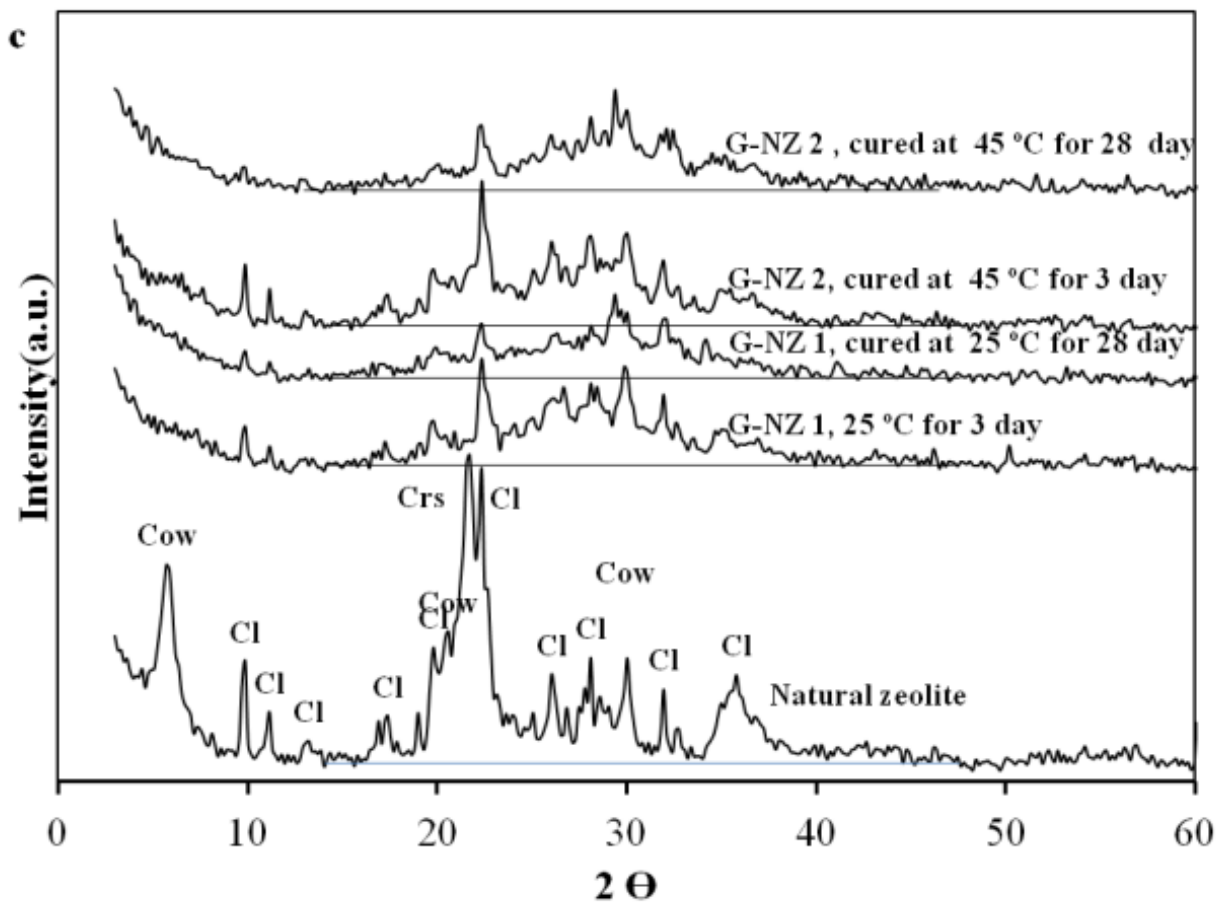
intensities of this band decrease with curing time and temperature and shifted to higher frequencies than that of original zeolite (Fig. 3e). The stretching vibration of carbonates, which formed during carbonation of geopolymer, appears at  $1382\text{ cm}^{-1}$  [52]. The peak ranged from  $2850\text{--}3700\text{ cm}^{-1}$  is related to stretching vibration of chemically compound water while the other peak at  $1611\text{--}1684\text{ cm}^{-1}$  is attributed to bending vibration of physically water [53]. The intensities of these peaks reduced with curing temperature as a result of evaporation of water.

The DSC curves of geopolymer cured for 3 and 28 days at ambient and  $45\text{ }^{\circ}\text{C}$  are illustrated

in Fig. 3e. These curves show only one characteristic endothermic peak ranged from  $55\text{--}175\text{ }^{\circ}\text{C}$  which is related to evaporation of free water and interstitial water in the geopolymer pores [54]. Other peaks can be that related to the thermal stability of geopolymer [55]. Fig. 3f shows SEM micrographs and EDX results for hardened geopolymer cured for 28 days and at ambient temperature. A dense matrix of geopolymerization overwhelmed the micrographs with modification of Si/Al ratio to 7.23 which indicates presence of geopolymer gel. In addition, some amount of Clinoptilolite appears.

**a**





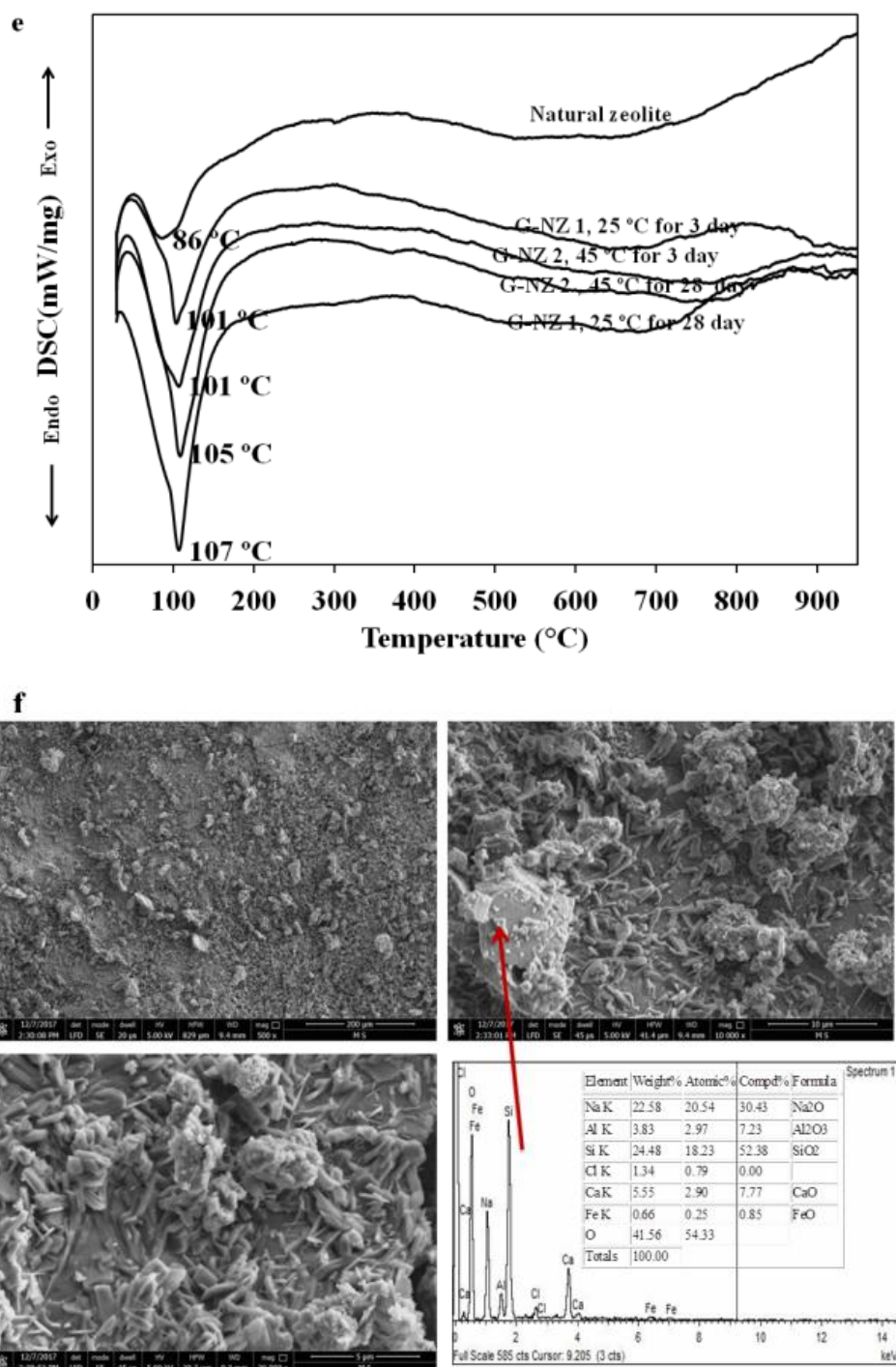


Fig. 3. (a) Photograph of prepared geopolymer, (b) Compressive strength of hardened geopolymer, (c) X-ray diffraction, (d) FTIR spectra, (e) DSC curve for hardened geopolymer cured at 25 °C and 45 °C, (f) SEM-EDX images of hardened geopolymer cured at 25 °C and 45 °C.

### 3.3. Characterization of NZ-Cement pastes

The average compressive strengths of cement pastes containing 0%, 5%, 10%, 15% and 20% of NZ cured up to 90 days are shown in Fig. 4a and Table 3. For all OPC paste and OPC-zeolite blended cement pastes, the hydration and pozzolanic reactions contributed to increase the compressive strength up to 90 days. OPC-NZ 10 has the highest compressive strength value in comparison to the reference paste (OPC). The strength activity index (SAI) (Fig. 4b) values show compressive strength for all OPC-NZ pastes higher than OPC at 3 days (29.0, 28.8, 18.6 and 119 % greater than OPC). However progressive hydration reduced values except for OPC-NZ 10. The increasing of strength in early age related to the filler effect of NZ that leads to accelerating the rate of cement minerals hydration. The dilution effect of cement is considered the main reason for reducing the compressive strength between 3 and 28 days, especially in the case of 20 % of NZ. In addition, the presence of  $\text{Na}^+$  and  $\text{K}^+$  ions that realized from NZ decreased the strength [56, 57].

Fig. 4c illustrates the XRD patterns of the blended samples with 0%, 5%, 10%, 15% and 20% of NZ cured for 28 days. Most of the hydration products have semi-amorphous nature except of portlandite. They showed only one crystalline product portlandite together the characteristics peaks of anhydrous clinker phases. As it is seen, the characteristic peaks of the portlandite ( $d \sim 4.90, 3.10, 2.62, 1.92, 1.79 \text{ \AA}$ ) decreased in intensity with increasing the NZ dose in the blended cement pastes, accompanied by decreasing the intensity of the distinctive peaks of anhydrous calcium silicate minerals ( $d \sim 3.02, 2.77, 2.6, 2.3 \text{ \AA}$ ). The characteristic peaks of zeolite appeared in samples OPC-NZ15 and OPC-NZ20 to indicate that still some amounts of zeolite did not react at this age of hydration. The increasing of background in the  $2\theta$  range  $25\text{--}35^\circ$  conformed presence of CSH [39].

Fig. 4c shows the heat flow of OPC and OPC-NZ blended cement cured for 28 days.

Only one endothermic effect appears in the range  $50\text{--}200 \text{ }^\circ\text{C}$  for NZ with an enthalpy  $22.5 \text{ J/g}$  that related to realizing of water. The DSC curves of OPC and blended cement show several thermal effects related to changing in sizes and shapes with the amount of the NZ. The endothermic peak at  $50\text{--}250 \text{ }^\circ\text{C}$  is due to liberation of physical water and dehydration of calcium silicate hydrate as the main hydration product of OPC. The amounts of different hydration phases in the hardened cement pastes can be determined from the enthalpy of the corresponding peak [58].

As shown from Fig. 4e and Table 3 the DSC peak temperature and enthalpy of CSH changed with the increasing the NZ content in the samples. The sample with 10 % NZ shows the highest enthalpy and the lowest CSH decomposition temperature. The second peak at the temperature range  $469\text{--}483 \text{ }^\circ\text{C}$  is connected with decomposition of portlandite ( $\text{Ca}(\text{OH})_2$ ) [59]. This peak shift to the lower temperature side with addition of NZ can be related to presence of disordered calcium hydroxide. In addition, the area of this peak decreased with the increases of amount of NZ as a result of pozzolanic reaction with zeolite [60]. The endothermic effect appears in  $680\text{--}780 \text{ }^\circ\text{C}$  is which can be devoted to the decomposition of calcium carbonate. The enthalpies of calcium carbonate for samples containing NZ are similar but less than those containing OPC.

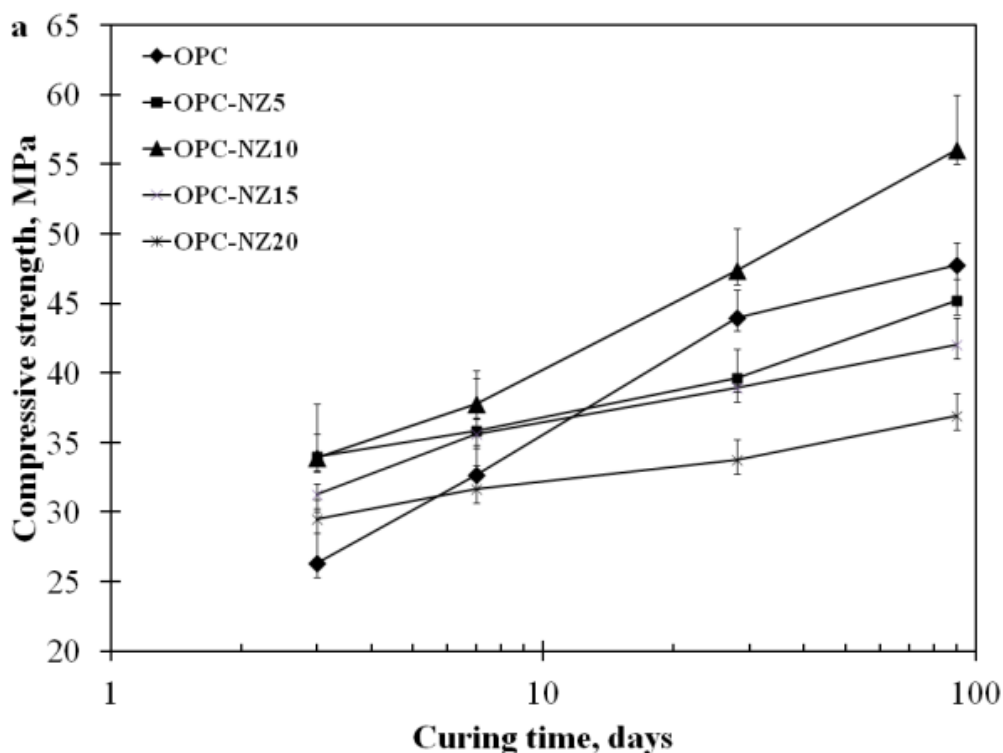
Fig. 4d illustrates the FTIR spectra of cement-zeolite pastes hydrated for 28 days. The band at  $3644 \text{ cm}^{-1}$  is related to the OH vibration (associated to CH), where there is a remarkable decrease of its intensity, especially for the sample loaded with 10 % of NZ and more. The decrease of this band confirms the reaction of NZ accordance of the pozzolanic reaction. The broad band at about  $3444 \text{ cm}^{-1}$  is attributed to the chemically bound water molecules while that at  $1637 \text{ cm}^{-1}$  to physically water. The adsorption bands of carbonates appear at  $1477$  and  $871 \text{ cm}^{-1}$  due to carbonation of samples during handling [61]. The main IR band at  $997 \text{ cm}^{-1}$  (for cement paste) demoted to Si-O

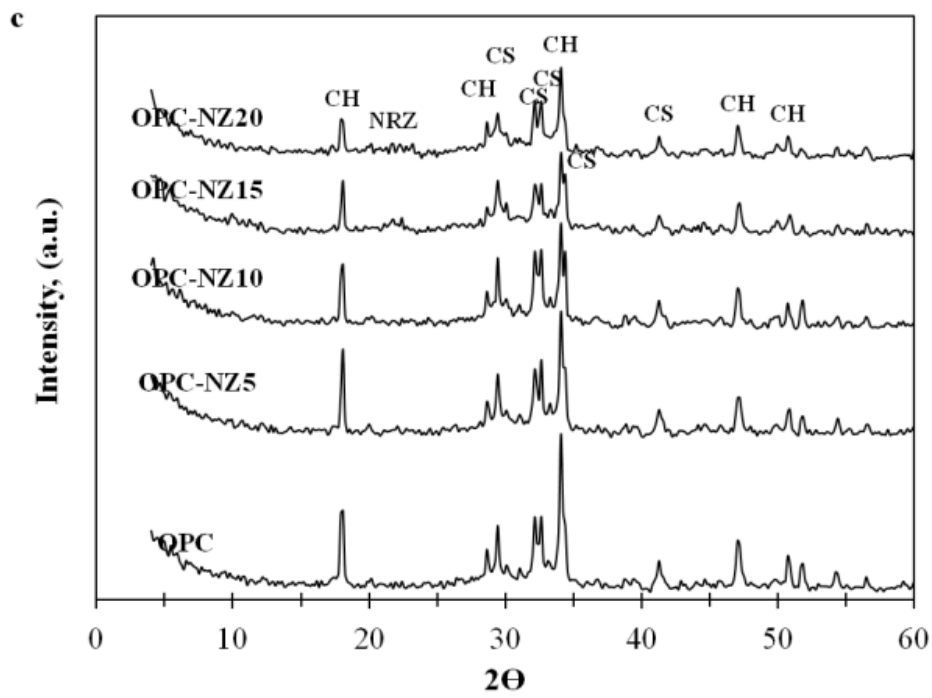
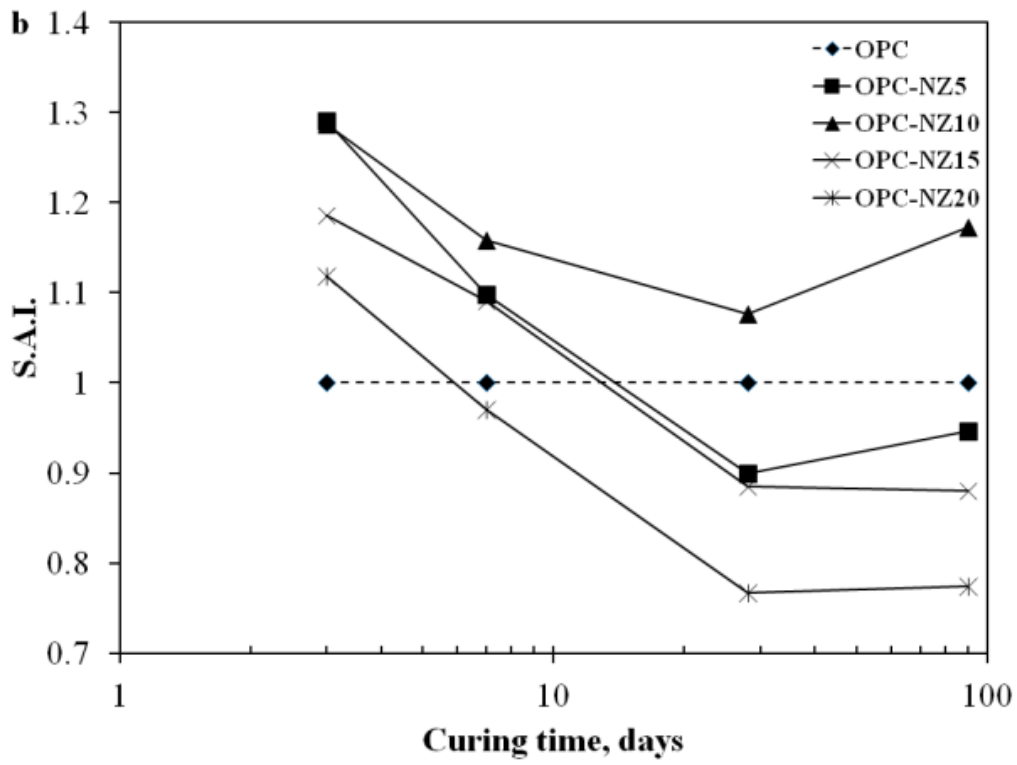
vibration for CSH. These bands could be changed in intensity and/or frequency with change of the Ca/Si ratio. This band is shifted to a lower frequency i.e.  $991\text{ cm}^{-1}$  with addition of 5% of NZ (OPC-NZ 5) while with increasing the NZ dose it is shifted to high-frequencies  $1029\text{ cm}^{-1}$ ,  $1029\text{ cm}^{-1}$  and  $1031\text{ cm}^{-1}$  for OPC-NZ 10, OPC-NZ 15 and OPC-NZ 20, respectively [62]. The hardened NZ-cement

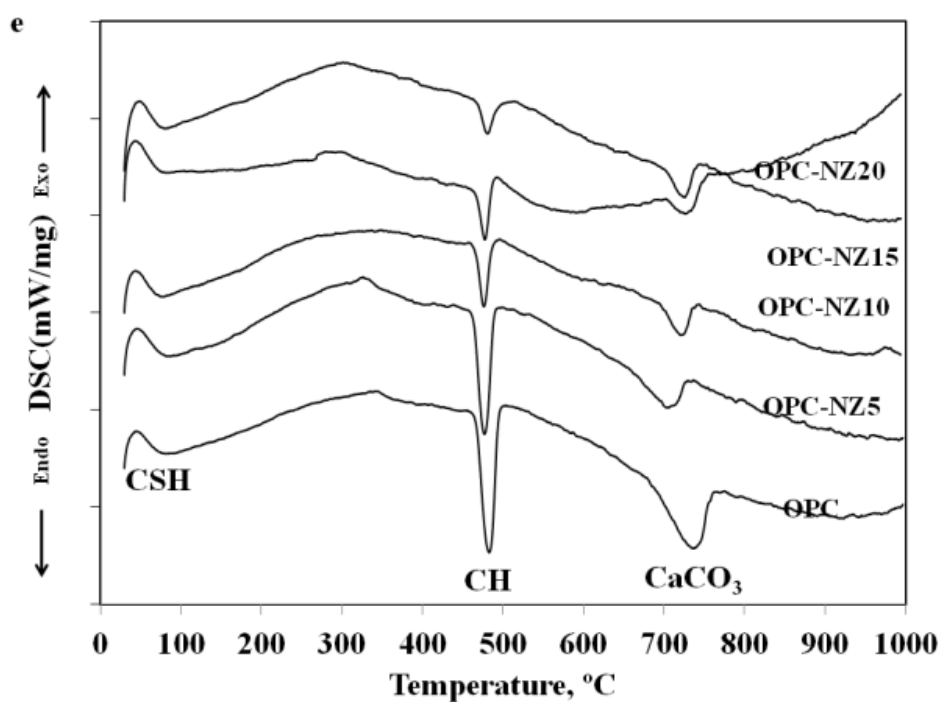
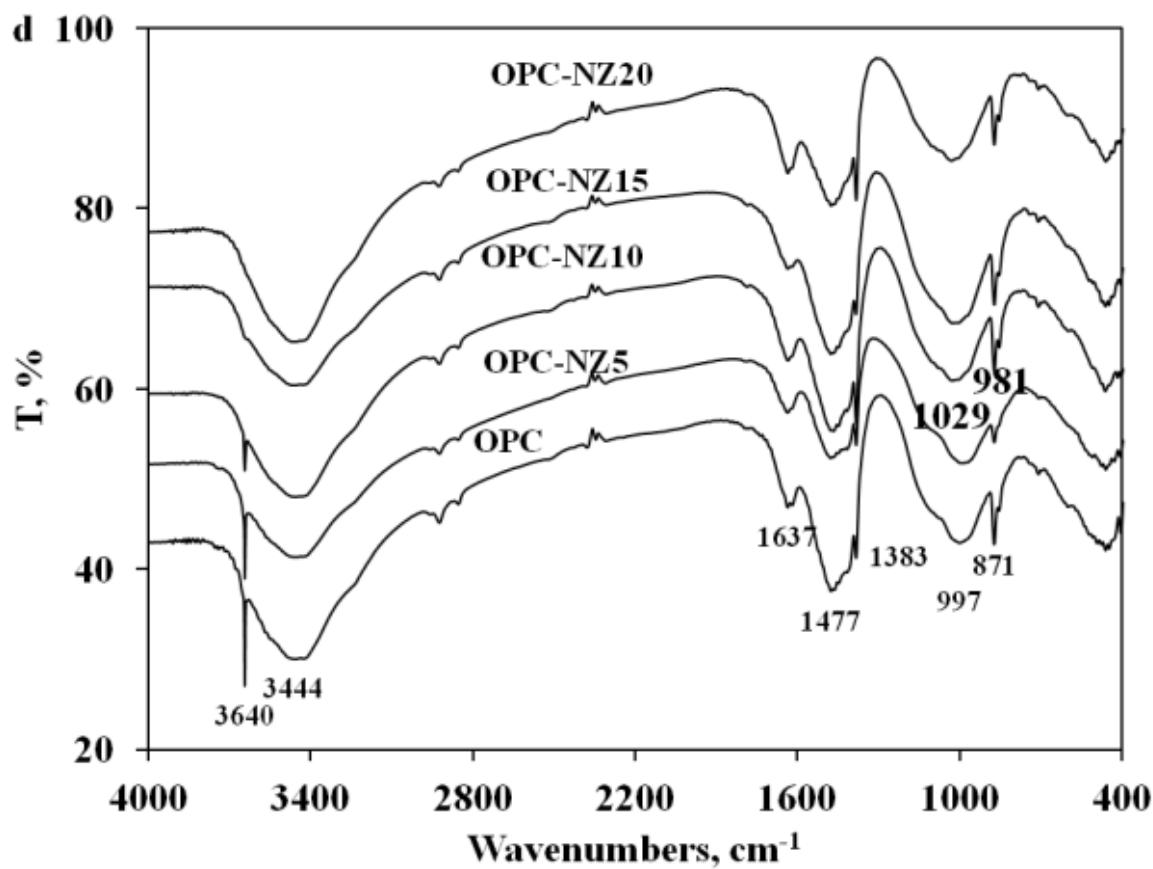
past (OPC-NZ10) cured for 28 days subjected to SEM - EDX analysis to examine its microstructure (Fig. 4f). The micrograph shows CSH crystals with a fibrous morphology [63]. The relating EDX spectrum given in Fig. 4f indicates that the Ca/Si =2 conforming the reaction occurring between NZ and portlandite [64].

**Table 3 : DSC peak temperature and enthalpy for zeolite blended samples cured for 28 days and 3- 28-day compressive strength up to 90 days.**

Peak	OPC		OPC-NZ5		OPC-NZ10		OPC-NZ15		OPC-NZ20	
	T(C)	J/g	T(C)	J/g	T(C)	J/g	T(C)	J/g	T(C)	J/g
CSH	82	29.9	85	27.3	78	32.6	81	24.9	82	24.2
CH	482	19.3	479	18.30	479	9.40	479	6.60	481	5.25
CaCO <sub>3</sub>	735	18.8	705	9.15	723	8.5	730	6.9	726	7.76
Crystallization	-	-	-	-	975	3.2	-	-	-	-
Compressive strength (MPa)										
3 days	26(3.69)		27(3.81)		34(1.69)		31(0.79)		29(1.39)	
7 days	33(5.30)		36(3.80)		38(2.38)		36(1.08)		32(1.69)	
28 days	44(2.00)		40(2.12)		47(3.06)		39(0.23)		34(1.51)	
90 days	48(1.62)		45(2.43)		56(4.00)		42(2.00)		37(1.62)	







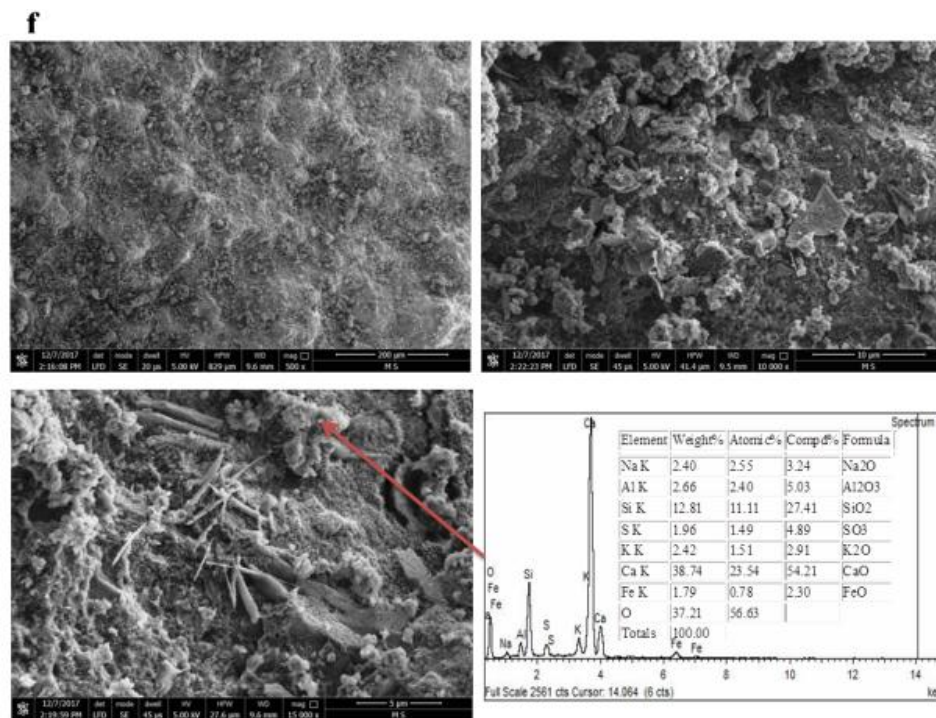


**Fig. 4. (a) Compressive strength of hardened cement-NZ pastes, (b) S.A.I., (c) X-ray diffraction, (d) FTIR spectra, (e) DSC curve, (f) SEM images of hardened OPC-NZ10 paste cured at 28 days.**

#### 4. CONCLUSIONS

The following conclusions are resulting from the study of natural raw zeolite as pozzolanic material for preparation of geopolymer and blended cement:

- According to ASTM C618 requirements, the natural raw zeolite from Harrat Shama (Tuffil) is a good pozzolanic material.
- It is composed of clinoptilolite, cowlesite and cristobalite and considered as clinoptilolite-zeolite class.
- The NZ reacted with activator solution to give a geopolymer matrix that has been conformed using XRD, FTIR, DSC, SEM-EDS results. The compressive strength of geopolymer paste is enhanced with increasing curing temperature.
- The addition of nature row zeolite to Portland cement accelerates the hydration of cement especially at early ages. The

incorporation of 10% by mass can be considered as a limit for its effective use. Above this limit, a substantial part of zeolite reduced compressive strength.

- Finally, we can be concluded that the natural raw zeolite needs to thermal activation in order to improve its pozzolanic activity.

#### REFERENCES

- [1] E. Papa, V. Medri, S. Amari, J. Manaud, P. Benito, A. Vaccari, E. Landi, Zeolite-geopolymer composite materials: production and characterization, *J. Cleaner Prod.*171 (2017)76-84.
- [2] G.J. Millar, S.J. Couperthwaite, K. Alyuz, Behaviour of natural zeolites used for the treatment of simulated and actual coal seam gas water, *J. Environ. Chem. Eng.* 4 (2016)1918-1928.

- [3] L.G. Messina, P.R. Bonelli, A.L. Cukierman, In-situ catalytic pyrolysis of peanut shells using modified natural zeolite, *Fuel. Process. Technol. Fuel Processing Technology*, 159 (2017)160-167.
- [4] L. Gómez-Hortigüela, J. Pérez-Pariente, R. García, Y. Chebude, I. Díaz, Natural zeolites from Ethiopia for elimination of fluoride from drinking water, *Sep. Purif. Technol.* 120 (2013) 224-229.
- [5] E. Saputra, M.A. Budihardjo, S. Bahri, J.A. Pinem, Cobalt-exchanged natural zeolite catalysts for catalytic oxidation of phenolic contaminants in aqueous solutions, *J. Water Process Eng.* 12 (2016) 47-51.
- [6] I. Sancho, E. Licon, C. Valderrama, N. de Arespacochaga, S. López-Palau, J.L. Cortina, Recovery of ammonia from domestic wastewater effluents as liquid fertilizers by integration of natural zeolites and hollow fibre membrane contactors, *Sci. Total Environ.* 584 (2017) 244-251.
- [7] I. Garcia-Lodeiro, A. Palomo, A. Fernández-Jiménez, F. Pacecho-Torgal, L.A. Labrincha, C. Leonelli, A. Palomo, P. Chindaprasirt, An overview of the chemistry of alkali-activated cement-based binders, *Handbook of Alkali-activated Cements, Mortars and Concretes*, p. 19 (UK) 2015.
- [8] J. Davidovits, *Geopolymers Chemistry and Applications*, Institut Geopolymere, Saint-Quentin, France, 2008.
- [9] J. Davidovits, Geopolymers—inorganic polymeric new materials, *J. Therm. Anal.* 37 (1991) 1633–1656.
- [10] C. Ferone, G. Roviello, F. Colangelo, R. Cioffi, O. Tarallo, Novel hybrid organic geopolymer materials, *Appl. Clay Sci.* 73 (2013) 42–50.
- [11] M. Babae, A. Castel, Chloride-induced corrosion of reinforcement in low-calcium fly ash-based geopolymer concrete, *Cement Concrete Res.* 88 (2016) 96-107.
- [12] C. Monticelli, M.E. Natali, A. Balbo, C. Chiavari, F. Zanotto, S. Manzi, C. Bignozzi, A study on the corrosion of reinforcing bars in alkali-activated fly ash mortars under wet and dry exposures to chloride solutions, *Cement Concrete Res.* 87 (2016) 53-63.
- [13] R.H. Haddad, O. Alshbuol, Production of geopolymer concrete using natural pozzolan: A parametric study, *Constr. Build. Mater.* 114 (2016) 699-707.
- [14] M. Sarkaret, K. Dana, S. Das, Microstructural and phase evolution in metakaolin geopolymers with different activators and added aluminosilicate fillers, *J. Mol. Struct.* 1098 (2015)110-118.
- [15] S. Andrejkovičová, A. Sudagar, J. Rocha, C. Patinha, W. Hajjaji, F. da Silva, F. Rocha, The effect of natural zeolite on microstructure, mechanical and heavy metals adsorption properties of metakaolin based geopolymers, *Appl. Clay Sci.* 126 (2016) 141-152.
- [16] A. Nikolov, I. Rostovsky, H. Nugteren, Geopolymer materials based on natural zeolite, *Case Stud. Constr. Mater.* 6 (2017)198-205.
- [17] W. Jo, S. Choi, K.W. Yoon, H. Park, Material characteristics of zeolite cement mortar, *Constr. Build. Mater.* 36 (2012) 1059-1065.
- [18] B. Ahmadi, M. Shekarchi, Use of natural zeolite as a supplementary cementitious material, *Cement Concrete Comp.* 32 (2010) 134-141.
- [19] F. Massazza, Properties and applications of natural pozzolanas, in: Barnes, P., Bensted, J., 2002. *Structure and performance of cements*. 2nd edition, Spon Press, London, 2001, pp. 326–352.
- [20] R. Madandoust, S.Y. Mousavi, Fresh and hardened properties of self-compacting concrete containing metakaolin, *Constr. Build. Mater.* 35 (2012)752-760.
- [21] A. Ramezani-pour, R. Mousavi, M. Kalhori, J. Sobhani, M. Najimi, Micro and macro level properties of natural zeolite contained concretes, *Constr. Build. Mater.* 101 (2015)347-358.
- [22] E. Vejmelková, D. Koňáková, T. Kulovaná, M. Keppert, J. Žumár, P. Rovnaníková, R. Černý, Engineering properties of concrete containing natural zeolite as supplementary cementitious material: Strength, toughness, durability, and hygrothermal performance, *Cement Concrete Comp.* 55 (2015)259-267.
- [23] S. Seraj, R.D. Ferron, M.C. Juenger, Calcining natural zeolites to improve their effect on cementitious mixture workability, *Cement Concrete Res.* 85(2016)102-110.
- [24] L.E. Burris, M.C. Juenger, Milling as a pretreatment method for increasing the reactivity of natural zeolites for use as supplementary cementitious materials, *Cement Concrete Comp.* 65(2016)163-170.
- [25] B. Uzal, L. Turanl, Blended cements containing high volume of natural zeolites: Properties,

- hydration and paste microstructure, *Cement Concrete Comp.* 34 (2012)101-109.
- [26] C. Karakurt, İ.B. Topçu, Effect of blended cements produced with natural zeolite and industrial by-products on alkali-silica reaction and sulfate resistance of concrete, *Constr. Build. Mater.* 25 (2011)1789-1795.
- [27] R. Snellings, G. Mertens, Ö. Cizer, J. Elsen, Early age hydration and pozzolanic reaction in natural zeolite blended cements: Reaction kinetics and products by in situ synchrotron X-ray powder diffraction. *Cement Concrete Res.* 40 (2010) 1704-1713.
- [28] V. Tydlitát, J. Zákoutský, R. Černý, Early-stage hydration heat development in blended cements containing natural zeolite studied by isothermal calorimetry, *Thermochim. Acta.* 582 (2014) 53-58.
- [29] D. Nagrockiene, G. Girskas, Research into the properties of concrete modified with natural zeolite addition, *Constr. Build. Mater.* 113 (2016) 964-969.
- [30] A. Dousti, R. Rashednia, B. Ahmadi, M. Shekarchi, Influence of exposure temperature on chloride diffusion in concretes incorporating silica fume or natural zeolite, *Constr. Build. Mater.* 49 (2013)393-399.
- [31] V. Lilkov, O. Petrov, D. Kovacheva, I. Rostovsky, Y. Tzvetanova, V. Petkova, N. Petrova, Carbonation process in cement with mineral additions of natural zeolite and silica fume—Early hydration period (minutes) up to 24 hours, *Constr. Build. Mater.* 124 (2016)838-845.
- [32] R.J. Stern, P. Johnson, Continental lithosphere of the Arabian Plate: a geologic, petrologic, and geophysical synthesis, *Earth Sci. Rev.* 101 (2010) 29-67.
- [33] A.A. Motelib, E.A. Khalaf, H. Al-Marzouki, Growth, destruction and facies architecture of effusive and explosive volcanics in the Miocene Shama basin, southwest of Saudi Arabia: Subaqueous–subaerial volcanism in a lacustrine setting, *J. Volcanol. Geoth. Res.* 309 (2016)156-177.
- [34] M.E.S.I. Saraya, E. El-Fadaly, Preliminary study of alkali activation of basalt: effect of NaOH concentration on geopolymerization of basalt. *J. Mater. Sci. Chem. Eng.* 5(11) (2017) 58.
- [35] M.E.S.I. Saraya, Stopping of cement hydration by various methods, *HBRC J.* 6 (2010) 36-60.
- [36] S.J. Kang, K. Egashira, A. Yoshida, Transformation of a low-grade Korean natural zeolite to high cation exchanger by hydrothermal reaction with or without fusion with sodium hydroxide, *Appl. Clay Sci.* 13(1998) 117-135.
- [37] C. ASTM, C618-08a: Standard Specification for Coal Fly Ash and Raw or Calcined Natural Pozzolan for Use in Concrete, *Annual Book of ASTM Standards*, (2008).
- [38] A. Chakchouk, B. Samet, T. Mnif, Study on the potential use of Tunisian clays as pozzolanic material, *Appl. Clay Sci.* 33 (2006)79-88.
- [39] T. Perraki, A. Orfanoudaki, Mineralogical study of zeolites from Pentalofos area, Thrace, Greece, *Appl. Clay Sci.* 25 (2004) 9-16.
- [40] K. Elaiopoulos, T. Perraki, E. Grigoropoulou, Mineralogical study and porosimetry measurements of zeolites from Scaloma area, Thrace, Greece, *Micropor. Mesopor. Mater.* 112 (2008) 441-449.
- [41] F. Rahmani, M. Haghighi, M. Amini, The beneficial utilization of natural zeolite in preparation of Cr/clinoptilolite nanocatalyst used in CO<sub>2</sub>-oxidative dehydrogenation of ethane to ethylene, *J. Ind. Eng. Chem.* 31 (2015)142-155.
- [42] T.N. Koltsova, Zeolites of the natrolite-thomsonite series, *Inorg. Mater.* 41 (2005)750-756.
- [43] Y. Foy, The crystal chemistry of cowlesite, *Mineral. Mag.* 56(1992) 575-579.
- [44] D. Zhao, K. Cleare, C. Oliver, C. Ingram, D. Cook, R. Szostak, L. Kevan, Characteristics of the synthetic heulandite-clinoptilolite family of zeolites, *Micropor. Mesopor. Mater.* 21 (1998) 371-379.
- [45] P. Castaldi, L. Santona, C. Cozza, V. Giuliano, C. Abbruzzese, V. Nastro, P. Melis, Thermal and spectroscopic studies of zeolites exchanged with metal cations, *J. Mol. Struct.* 734 (2005)99-105.
- [46] M. Mohamed, Heat capacities, phase transitions and structural properties of cation-exchanged H-mordenite zeolites, *Thermochim. Acta.* 372 (2001)75-83.
- [47] B.E. Alver, M. Sakizci, E. Yörükoğullari, Investigation of clinoptilolite rich natural zeolites from Turkey: a combined XRF, TG/DTG, DTA and DSC study, *J. Therm. Anal. Calorim.* 100 (2010)19-26.

- [48] O. Korkuna, R. Leboda, J. Skubiszewska-Zie, T. Vrublevs'ka, V.M. Gunko, J. Ryczkowski, Structural and physicochemical properties of natural zeolites: clinoptilolite and mordenite. *Micropor. Mesopor. Mater.* 87 (2006)243-254.
- [49] T. Markiv, K. Sobol, M. Franus, W. Franus, Mechanical and durability properties of concretes incorporating natural zeolite, *Arch. Civ. Mech. Eng.* 16 (2016)554-562.
- [50] E. Xingu-Contreras, G. García-Rosales, I. García-Sosa, A. Cabral-Prieto, M. Solache-Ríos, Characterization of natural zeolite clinoptilolite for sorption of contaminants, *Hyperfine Interact.* 232 (2015)7-18.
- [51] S.K. Nath, S. Kumar, Influence of iron making slags on strength and microstructure of fly ash geopolymer, *Constr. Build. Mater.* 38 (2013) 924-930.
- [52] D. Panias, I. P. Giannopoulou, T. Perraki, Effect of synthesis parameters on the mechanical properties of fly ash-based geopolymers, *Colloid. Surface. A.* 301 (2007) 246-254.
- [53] K. Boonserm, V. Sata, K. Pimraksa, P. Chindaprasirt, Improved geopolymerization of bottom ash by incorporating fly ash and using waste gypsum as additive, *Cement Concrete Comp.* 34 (2012)819-824.
- [54] A. Buchwald, M. Vicent, R. Kriegel, C. Kaps, M. Monzó, A. Barba, Geopolymeric binders with different fine fillers—phase transformations at high temperatures, *Appl. Clay Sci.* 46 (2009)190-195.
- [55] T.W. Cheng, J.P. Chiu, Fire-resistant geopolymer produced by granulated blast furnace slag, *Miner. Eng.* 16(2003) 205-210.
- [56] I. Jawed, J. Skalny, Alkalies in cement: a review: II. Effects of alkalies on hydration and performance of Portland cement, *Cement Concrete Res.* 8(1978)37-51.
- [57] A. Rivera, G. Rodriguez-Fuentes, E. Altshuler, Time evolution of a natural clinoptilolite in aqueous medium: conductivity and pH experiments, *Micropor. Mesopor. Mater.* 40 (2000)173-179.
- [58] W. Sha, G.B. Pereira, Differential scanning calorimetry study of ordinary Portland cement paste containing metakaolin and theoretical approach of metakaolin activity, *Cement Concrete Comp.* 23 (2001)455-461.
- [59] P. Esteves, On the hydration of water-entrained cement–silica systems: combined SEM, XRD and thermal analysis in cement pastes, *Thermochim. Acta* 518 (2011) 27-35.
- [60] A. Trník, L. Scheinherrová, I. Medved', R. Černý, Simultaneous DSC and TG analysis of high-performance concrete containing natural zeolite as a supplementary cementitious material. *J. Therm. Anal. Calorim.* 121, (2015) 67-73.
- [61] V. Villa, R. Fernández, O. Rodríguez, R. García, E. Villar-Cociña, M. Frías, Evolution of the pozzolanic activity of a thermally treated zeolite. *J. Mater. Sci.* 48(2013)3213-3224.
- [62] T. Milović, M. Radeka, M. Malešev, V. Radonjanin, Compressive strength and mineralogical properties of cement paste containing zeolite. In *International conference contemporary achievements in civil engineering* 22 (2016)397-403.
- [63] L. Scrivener, Backscattered electron imaging of cementitious microstructures: understanding and quantification, *Cement Concrete Comp.* 26 (2004)935-945.
- [64] J.J. Thomas, H.M. Jennings, A.J. Allen, Relationships between Composition and Density of Tobermorite, Jennite, and Nanoscale CaO– SiO<sub>2</sub>– H<sub>2</sub>O, *J. Phys. Chem. C.* 114 (2010)7594-76010..